  Bull. Chem. Soc. Jpn., 62, 2362—2368 (1989) [Vol. 62, No. 7

Multi-Ionic Potential and Membrane Permeability Matrix. III. Diffusion and Concentration of Ions within Membrane Phase as a Controlling Factor to Ion Permselectivity

Kozue KAIBARA,* Hiroyoshi INOUE, and Toshio ARITOMI
Department of Chemistry, Faculty of Science, Kyushu University,
Hakozaki, Higashi-ku, Fukuoka 812
(Received February 15, 1989)

Membrane concentrations of cations in the NaCl–CsCl and NaCl–$CaCl_2$ systems with a highly selective cation-exchange membrane were measured under the extensive external electrolyte conditions. The modes of membrane/solution distribution and diffusion of cations, as a controlling factor to the membrane permselectivity, were correlated consistently with the electrochemical and cation flux data, as well as with the estimated membrane permselectivity parameters. The NaCl–CsCl uni-uni valent cation system was characterized well by the Na^+/Cs^+ concentration ratio of external solution, since the Na^+/Cs^+ concentration ratio in the membrane phase was related directly to the external ratio. Na^+/Cs^+ diffusion coefficient ratio varied from 0.5 to 3 with increasing external Na^+/Cs^+ concentration ratio from 1/100 to 100. While in the NaCl–$CaCl_2$ uni-bi valent cation system, the high and constant membrane concentration of Ca^{2+} regulated the transport process. The Na^+/Ca^{2+} diffusion coefficient ratio ranged from 0.5 to 500 with external Na^+/Ca^{2+} ratio from 1/100 to 100. Analyses on the phenomenological coefficients, describing the inter-cationic correlations within the membrane phase, as a function of the external cation concentration ratio were also carried out.

Selective ion transport processes across a charged-membrane are controlled, in general, by the modes of ionic migration within the membrane phase and by the profiles of ionic distribution between the membrane and external phases (see e.g., Refs. 1—3). Therefore, the phenomenological studies of the membrane transport process, such as the measurements of transmembrane potential, conductance, and ion flux, as well as the estimations of membrane transport parameters describing the permeability and selectivity to permeant ions, must be consistent with the results on the estimations of ionic behaviors within the membrane phase. The aim of the present experiments is to examine the conditions of permeant ions within the membrane phase and to correlate these results systematically with the results based on the linear phenomenological analyses in the multi-ionic transport systems with a cation-exchange membrane.[4,5] The substantial ion permselectivity of an ion-exchange membrane should be evaluated in the multiple counterion systems and the practical ion-exchange membrane related techniques are operated usually in a multi-ionic system as in the sea water condensation process (see e.g., Refs. 6—9). The present experiments are designed not only for the detailed phenomenological descriptions of the multi-ionic membrane transport process but also for the survey of a more efficient operating condition in the ion-exchange membrane-related processes.

Experimental

A typical highly selective cation-exchange membrane, CK-1,1.0t (Asahi Chemical Industry Co., Ltd.), was used throughout the present experiments. The basic physicochemical properties of the CK-1, 1.0t membrane were noted in earlier papers.[4,5,10] Electrolyte solutions were prepared from extra pure salts with twice-distilled water. All the measurements were carried out at regulated room temperature, 25±1 °C.

In the present experiments, the membrane properties were examined in NaCl–CsCl and NaCl–$CaCl_2$ systems, where the concentration of one of the electrolytes is varied from 10^{-1} to 10^{-3} mol dm^{-3} and that of the other electrolyte is kept constant at 10^{-1}, 10^{-2}, or 10^{-3} mol dm^{-3}. Then, the concentration ratios of the two kinds of external electrolytes ranged at 100—1/100. In case of the CK-1, 1.0t membrane, the previous experimental results on the single electrolyte systems indicated that the cation concentrations within the membrane phase are almost constant at below the external electrolyte concentration of around 5×10^{-1} mol dm^{-3} and, above this external concentration, rapid increases in the membrane cation concentration due to a drastic intrusion of Donnan adsorbed cations are observed.[10] Accordingly in the present experimental conditions, it is expected that the total cation concentrations in the membrane phase are kept at a constant level and that the effects of relative occupancy of respective cations for available membrane sites upon the membrane transport process can be examined systematically.

Membrane concentrations of the respective cations were measured by the following procedures. A piece of the CK-1, 1.0t membrane sample (0.1—0.2 g, ca.1 cm^2), preweighed at the reference conditions in which all the membrane samples were equilibrated sufficiently with 10^{-1} mol dm^{-3} NaCl solution, was immersed in the test aqueous solution with an appropriate electrolyte composition for 96 h to establish sufficiently an equilibrium condition of ions within the membrane phase. Then the test membrane sample, being wiped off the adhering electrolyte solution, was washed with distilled water for 72 h to extract Donnan adsorbed ions. It was required at least 50 h to elute stiffly adsorbed Donnan ions in the CK-1, 1.0t membrane. In the next step, remaining cations which are thought to be bound to ion-exchange sites were extracted perfectly by means of soaking the membrane sample into 1 mol dm^{-3} HCl solution for 24 h. Cation concentrations in the respective aqueous eluents were measured with an atomic absorption spectrophotometer (Hitachi 180-50) after the suitable dilution

steps and/or, in case of the bi-cationic systems, the appropriate treatments to prevent from the interference due to the coexisting cations. The Cs^+ concentrations were measured with addition of $CaCl_2$ into the eluent sample solutions to inhibit the ionizations of Cs and to increase the spectral intensities.

Electrochemical measurements to estimate the transmembrane potential and conductance data as well as intercompartmental cation flux measurements were described in earlier papers.[4,5] The experimental systems consisted of aqueous solution phases I and II separated by the membrane, one of which contains NaCl as electrolyte and the other, CsCl or $CaCl_2$. The concentration of one of the electrolytes in phase I was varied from 10^{-1} to 10^{-3} mol·dm^{-3} and that of the other electrolyte in phase II was kept constant at 10^{-1}, 10^{-2}, or 10^{-3} mol dm^{-3}. The respective electrolyte concentrations in phases I and II correspond to those in the systems for the membrane ion concentration measurements described above. As will be discussed in the later section, the membrane-electrolyte solution systems in the present study are close fairly to the cationic equilibrium condition, so the experimental data obtained from the two types of the systems, the binary (two counterion) systems equilibrated or separated with a cation-exchange membrane, are correlated well to each other.

Results and Discussion

Thermodynamic background for the analyses of the present membrane transport process can be summarized as follows. When Z_1-valent metal, M_1, and Z_2-valent metal M_2 in chloride form are dissolved in the aqueous phases I and II separated by the membrane phase, respectively, the fundamental linear phenomenological equation employing the membrane permeability matrix as a principal transport parameter is expressed as:[4,5]

$$\begin{bmatrix} J_{M_1} \\ J_{M_2} \\ J_{Cl} \end{bmatrix} = - \begin{bmatrix} P_{M_1\cdot M_1} & P_{M_1\cdot M_2} & P_{M\cdot Cl} \\ P_{M_2\cdot M_1} & P_{M_2\cdot M_2} & P_{M_2\cdot Cl} \\ P_{Cl\cdot M_1} & P_{Cl\cdot M_2} & P_{Cl\cdot Cl} \end{bmatrix} \begin{bmatrix} -a^{I}_{M_1}\exp(-Z_1FV/2RT) \\ a^{II}_{M_2}\exp(Z_2FV/2RT) \\ a^{II}_{Cl}\exp(-FV/2RT) - a^{I}_{Cl}\exp(FV/2RT) \end{bmatrix} \quad (1)$$

where J is the ionic flux, a is the activity, V is the membrane potential, F is the Faraday constant, R is the gas constant, and T is the absolute temperature; the subscripts M_1, M_2, and Cl refer to metal cations, M_1 and M_2, and chloride ion; the superscripts I and II indicate the solution phase. The 3×3 matrix in the right hand side of Eq. 1 is the membrane permeability matrix, of which elements represent the partial contributions of the inter-ionic correlations indicated by the subscript indices on the membrane transport processes. The respective matrix elements can be estimated based on the membrane potential, conductane, and ion flux data.[4,5] Since the electroconductive membrane permeabilities to metal cations M_1 and M_2 and to Cl^-, P_{M_1}, P_{M_2}, and P_{Cl}, are defined as a function of the membrane permeability matrix elements:

$$\begin{aligned} P_{M_1} &= P_{M_1\cdot M_2} + (Z_2P_{M_2\cdot M_1} - P_{Cl\cdot M_1})/Z_1 \\ P_{M_2} &= P_{M_2\cdot M_2} + (Z_1P_{M_1\cdot M_2} - P_{Cl\cdot M_2})/Z_2 \\ P_{Cl} &= P_{Cl\cdot Cl} - (Z_1P_{M_1\cdot Cl} + Z_2P_{M_2\cdot Cl}) \end{aligned} \quad (2)$$

the membrane electric current, I, is expressed as:

$$\begin{aligned} I &= F(Z_1J_{M_1} + Z_2J_{M_2} - J_{Cl}) \\ &= [FZ_1P_{M_1}a^{I}_{M_1}\exp(-Z_1FV/2RT) \\ &\quad - FZ_2P_{M_2}a^{II}_{M_2}\exp(Z_2FV/2RT)] \\ &\quad + FP_{Cl}[a^{II}_{Cl}\exp(-FV/2RT) - a^{I}_{Cl}\exp(FV/2RT)] \end{aligned} \quad (3)$$

The electroconductive membrane permeabilities to respective ions can be estimated directly from the electrochemical data such as the membrane potentials and conductances.[4,5,11]

Introducing the membrane permeability to whole cations, $P_{M_1\text{-}M_2}$, defined as:

$$P_{M_1\text{-}M_2} = (Z_1P_{M_1}Z_2P_{M_2})^{1/2}\exp[-(Z_1 - Z_2)FV/4RT] \quad (4)$$

the cationic component of membrane electric current, the term in the first brackets in Eq. 3, can be modified and the expression for the membrane electric current is reduced to:

$$\begin{aligned} I &= -2FP_{M_1\text{-}M_2}(a^{I}_{M_1}a^{II}_{M_2})^{1/2}\sinh[(Z_1 + Z_2)F(V - V_{M_1\text{-}M_2})/4RT] \\ &\quad + 2FP_{Cl}(a^{I}_{Cl}a^{II}_{Cl})^{1/2}\sinh[-F(V - V_{Cl})/2RT] \end{aligned} \quad (5)$$

where $V_{M_1\text{-}M_2}$ is the cationic equilibrium membrane potential, which corresponds to the Nernstian equilibrium potential for a single cationic system, and V_{Cl} is the Nernstian equilibrium membrane potential for Cl^-. The expression for $V_{M_1\text{-}M_2}$ is derived from Eq. 3 by introducing the conditions, I=0 and P_{Cl}=0 as:

$$V_{M_1\text{-}M_2} = -[2RT/(Z_1 + Z_2)F]\ln(Z_2P_{M_2}a^{II}_{M_2}/Z_1P_{M_1}a^{I}_{M_1}) \quad (6)$$

Equation 6 deduces that the linear relationships of $V_{M_1\text{-}M_2}$ with logarithmic $a^{I}_{M_1}$ correspond to the constant P_{M_1}/P_{M_2}. The transmembrane potential in the absence of electric current, V_0, is related to $V_{M_1\text{-}M_2}$ and V_{Cl} as:

$$V_0 = t_{M_1\text{-}M_2}V_{M_1\text{-}M_2} + t_{Cl}V_{Cl} \quad (7)$$

where $t_{M_1\text{-}M_2}$ and t_{Cl} are the transport numbers to the whole metal cations and Cl^-, respectively.

The membrane permselectivity to ions depends, in general, upon the membrane/solution distribution and migration speed of permeating ions.[1-3] The membrane permeability ratio of cations, P_{M_1}/P_{M_2}, can be expressed as:[4,12,13]

$$\frac{P_{M_1}}{P_{M_2}} = \frac{D^m_{M_1}}{D^m_{M_2}} \frac{C^m_{M_1,Total}/C^m_{M_2,Total}}{C^s_{M_1}/C^s_{M_2}} \quad (8)$$

where D^m is the diffusion coefficient of metal cation within the membrane phase and, C^m and C^s are the cation concentrations in the membrane phase and in the external solution, respectively. The total membrane concentration of metal cation M, $C^m_{M,Total}$, is the sum of two components of cation concentration within the membrane phase as:

$$C^m_{M_i,Total} = C^m_{M,H_2O} + C^m_{M,HCl} \quad (9)$$

where C^m_{M,H_2O} is the Donnan adsorbed component of metal cation M eluted with distilled water and $C^m_{M,HCl}$ is the site-bound component of metal cation M eluted with HCl solution as described in the experimental section. In the present study, changes in $C^m_{M,Total}$, C^m_{M,H_2O}, and $C^m_{M,HCl}$ for Na^+, Cs^+, and Ca^{2+} were measured as a function of the concentration and composition of external electrolyte solution. The respective components of the membrane cation concentrations are expressed in the unit of mol per kg of wet membrane sample in the reference conditions. Correlations of the membrane cation concentration with the membrane transport phenomena, such as the transmembrane potentials and ion fluxes, were examined systematically in the following part of this section.

C^m_{M,H_2O} and $C^m_{M,HCl}$ as a Function of the External Electrolyte Concentration. Figure 1 illustrates the Na^+ and Cs^+ concentrations within the CK-1, 1.0t membrane phase as a function of the external electrolyte concentration for the NaCl-CsCl systems, in which the concentration of NaCl or CsCl was varied from 10^{-1} to 10^{-3} mol dm^{-3} and that of the other electrolyte was kept constant at 10^{-2} mol dm^{-3}. As a result of the fact that 85—99% of Na^+ and more than 99% of Cs^+ were bound to the ion-exchange sites, the total site-bound cations, which should be constant and equivalent to the exchange capacity, came up to 98—99% of the total cations in the membrane phase, and accordingly Cl^- ions were almost perfectly excluded from the membrane phase. When the external NaCl and CsCl concentrations were the same, i.e., $C^s_{NaCl} = C^s_{CsCl} = 10^{-2}$ mol dm^{-3}, the concentration of the site-bound Cs^+ was as twice as that of the site-bound Na^+, so that $C^m_{Na,HCl}/C^m_{Cs,HCl} \cong 1/2$. Under the external condition, $C^s_{NaCl}/C^s_{CsCl} \cong 2.5$, the equivalent amounts of Na^+ and Cs^+ were bound to the ion-exchange sites, i.e., $C^m_{Na,HCl} = C^m_{Cs,HCl}$. The Donnan adsorbed cation component contained more Na^+ than Cs^+ in the external concentration range studied, for example, $C^m_{Na,H_2O}/C^m_{Cs,H_2O} \cong 1.4$ when $C^m_{NaCl} = C^s_{CsCl} = 10^{-2}$ mol dm^{-3} and $C^m_{Na,H_2O}/C^m_{Cs,H_2O} \cong 2$, when $C^s_{NaCl}/C^s_{CsCl} \cong 2.5$.

In case of the systems where Ca^{2+} permeates across the CK-1, 1.0t cation-exchange membrane, the membrane/solution distributions of Na^+ and Ca^+ were entirely different from those of Na^+ and Cs^+. Figure 2 summarizes the Donnan adsorbed and site-bound cation concentrations of Na^+ and Ca^{2+} for the

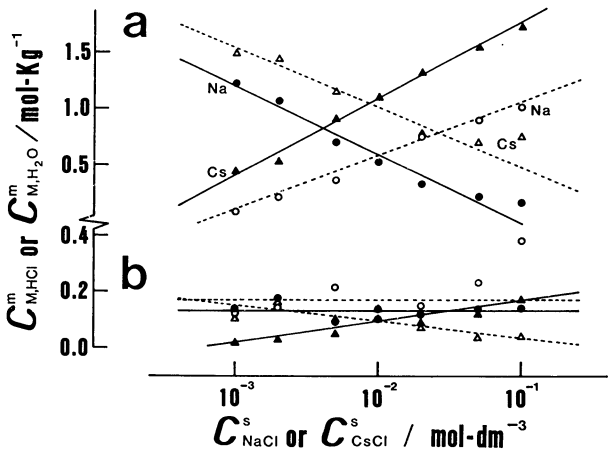

Fig. 1. Concentrations of the site-bound and Donnan adsorbed fractions of cations, Na^+ and Cs^+, in NaCl-CsCl systems. Concentrations within the membrane phase, $C^m_{M,HCl}$ and C^m_{M,H_2O}, as a function of the external electrolyte concentration, C^s_{NaCl} or C^s_{CsCl} equilibrated with the membrane phase. Upper frame a indicates $C^m_{M,HCl}$ and lower frame b indicates C^m_{M,H_2O}. ●: Na^+, ▲: Cs^+ in 10^{-2} mol dm^{-3} C^s_{NaCl} system. ○: Na^+, △: Cs^+ in 10^{-2} mol dm^{-3} C^s_{CsCl} system.

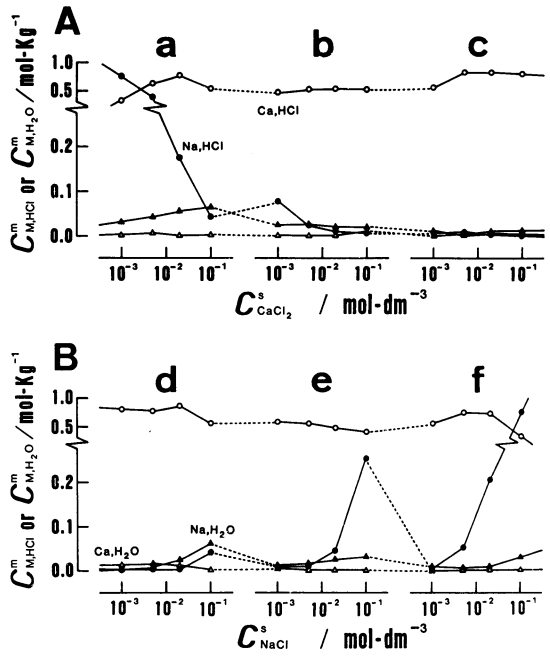

Fig. 2. Concentrations of the site-bound and Donnan adsorbed fractions of cations, Na^+ and Ca^{2+}, in NaCl-$CaCl_2$ systems. Concentrations within the membrane phase, $C^m_{M,HCl}$ and C^m_{M,H_2O}, as a function of the external electrolyte concentration, C^s_{NaCl} or $C^s_{CaCl_2}$. Constant C^s_{NaCl} system (A) and constant $C^s_{CaCl_2}$ system (B). C^s_{NaCl}, a: 10^{-1}; b: 10^{-2}; c: 10^{-3} mol dm^{-3}. $C^s_{CaCl_2}$, d: 10^{-1}; e: 10^{-2}; f: 10^{-3} mol dm^{-3}. ●: C^m_{NaHCl}, ○: $C^m_{Ca,HCl}$, ▲: C^m_{Na,H_2O}, △: C^m_{Ca,H_2O}.

$NaCl$–$CaCl_2$ systems, in which the external concentration of NaCl or $CaCl_2$ was varied from 10^{-1} to 10^{-3} mol dm^{-3} and that of the other electrolyte was kept constant at 10^{-1}, 10^{-2}, or 10^{-3} mol dm^{-3}. As can be seen in Fig. 2, the site-bound Ca^{2+} amounted to 97—99% of the total Ca^{2+} within the membrane phase keeps almost constant level. On the other hand, the site-bound Na^+ is varied from 15 to 96% of the total Na^+ in the membrane phase. In the external condition, $C^s_{NaCl}/C^s_{CaCl_2}<10$, the site-bound Ca^{2+} amounted to 80—98% of the total membrane cations. The concentrations of Donnan adsorbed Na^+ were 10 times larger than those of Ca^{2+}, when the external NaCl and $CaCl_2$ concentrations are the same, $C^s_{NaCl}=C^s_{CaCl_2}=10^{-1}$, 10^{-2}, or 10^{-3} mol dm^{-3}.

Membrane/Solution Distribution of Cations and Membrane Transport Phenomena. Quantitative and qualitative differences in the membrane/solution distribution of cations between the NaCl–CsCl and the NaCl–$CaCl_2$ systems cause characteristic and distinctive membrane transport phenomena in these systems. Figure 3 shows the correlations of the total cation concentration in the CK-1, 1.0t membrane (Fig. 3-C) with the membrane potential (Fig. 3-A) and inter-compartmental ion flux (Fig. 3-B) data for the NaCl–CsCl systems as a function of the external NaCl/CsCl concentration ratio. The total membrane concentrations of Na^+ and Cs^+, $C^m_{Na,Total}$ and $C^m_{Cs,Total}$, changed as the external Na^+ and Cs^+ concentrations, C^s_{NaCl} and C^s_{CsCl}, changed. $C^m_{Na,Total}$, was almost equal to $C^m_{Cs,Total}$ when $C^s_{NaCl}/C^s_{CsCl}=2.5$. These results indicate that the membrane affinities to Cs^+ are higher than those to Na^+. It is suggested that the higher membrane affinities to Cs^+ arise partly from accessibilities of Cs^+ to the fixed cation-exchange sites due to smaller hydrated radius of Cs^+ than that of Na^+. Under the external conditions where C^s_{NaCl}/C^s_{CsCl} ratios are lower than 1/10 or higher than 100, available exchange-sites were occupied by a large amount of Cs^+ or Na^+, respectively (see also Fig. 7-B).

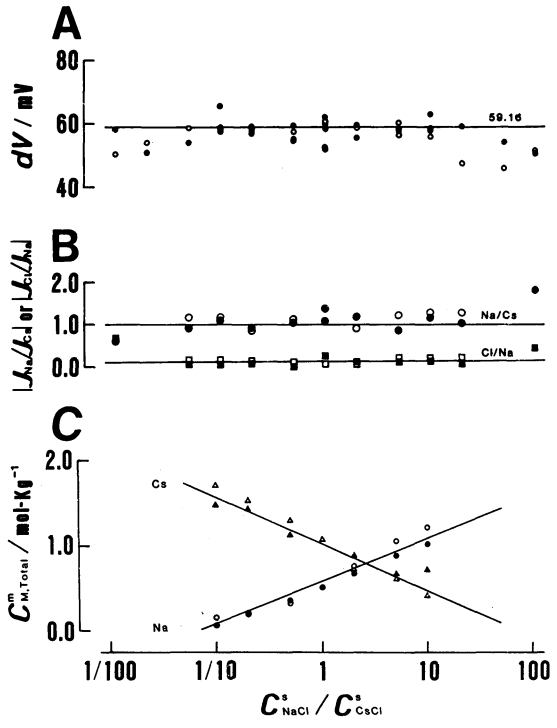

Fig. 3. Membrane potential gradient (for details see text), dV, inter-compartmental ionic flux ratio, $|J_{Na}/J_{Cs}|$ or $|J_{Cl}/J_{Na}|$, and total metal cation concentration within the membrane phase, $C^m_{Na,Total}$ or $C^m_{Cs,Total}$, as a function of external NaCl/CsCl concentration ratio, C^s_{NaCl}/C^s_{CsCl}. Closed and open marks indicate the constant C^s_{NaCl} and C^s_{CsCl} systems, respectively. These constant external electrolyte concentrations correspond to the constant electrolyte concentration in phase II separated from phase I by the membrane. In B, ● and ○: $|J_{Na}/J_{Cs}|$, ■ and □: $|J_{Cl}/J_{Na}|$. In C, ● and ○: $C^m_{Cs,Total}$, ▲ and △: $C^m_{Na,Total}$.

The transmembrane potential data are plotted as the gradient of the potential vs. logarithm of the mean electrolyte activity of phase I curve, dV ($=\Delta V/\Delta \log a^I_{M_1}$), in Fig. 3-A. It was suggested, on the basis of experimental results showing the almost perfect exclusion of Cl^- from the membrane phase, that the membrane process in the NaCl–CsCl system is controlled only by cations, Na^+ and Cs^+. In that case, the transmembrane potentials for the NaCl–CsCl systems are expected to be nearly equal to $V_{Na\text{-}Cs}$ and, accordingly, the estimated dV values should be close to 59.16 mV at 25 °C with the constant cationic permeability ratio, P_{Na}/P_{Cs}, as seen in Fig. 3-A (refer to Eq. 6). The inter-compartmental ion flux data also support these situations. As can be seen in Fig. 3-B, the Cl^- flux is suppressed at an extremely low level and the membrane transport process can be characterized by the Na^+ and Cs^+ fluxes in opposite directions with each other.

For the NaCl–$CaCl_2$ systems, the ideal uni- and bivalent cationic equilibrium potential, $V_{Na\text{-}Ca}$, is 39.44 mV at 25 °C as calculated from Eq. 6 with the constant P_{Na}/P_{Ca}. As can be seen in Fig. 4-A, the potential gradient dV values correspond to the ideal $V_{Na\text{-}Ca}$ values within the external electrolyte concentration range, $1/10<C^s_{NaCl}/C^s_{CaCl_2}<10$. However, the estimated dV values deviate positively or negatively in the external conditions where $C^s_{NaCl}/C^s_{CaCl_2}$ is higher than 10 or lower than 1/10, respectively. Corresponding to these transmembrane potential responses, the inter-compartmental ion fluxes varied in multiple modes. It is shown in Fig. 4-B that Cl^- flux is negligible in the range of $1/10<C^s_{NaCl}/C^s_{CaCl_2}<10$, so the Na^+ and Ca^{2+} fluxes flowing in opposite directions from each other control the transport processes across the CK-1, 1.0t cation-exchage membrane in the same manner as the above NaCl–CsCl systems are controlled only by Na^+ and Cs^+ fluxes. Out of this concentration range, the Na^+ and Cl^- fluxes increased with increasing relative concentration of external Na^+, whereas the Ca^{2+} and

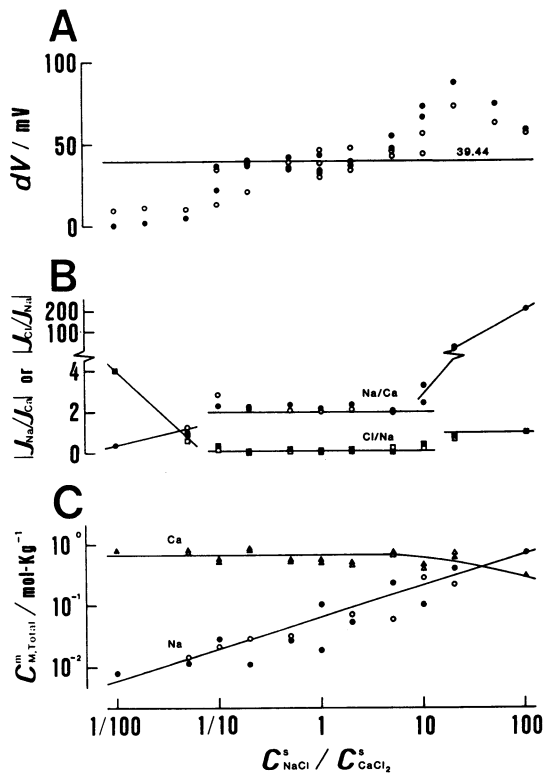

Fig. 4. Membrane potential gradient, dV, ionic flux ratio, $|J_{Na}/J_{Ca}|$ or $|J_{Cl}/J_{Na}|$, and total metal cation concentration within the membrane phase, $C^m_{Na,Total}$ or $C^m_{Ca,Total}$, as a function of the external NaCl/$CaCl_2$ concentration ratio, $C^s_{NaCl}/C^s_{CaCl_2}$. Closed and open marks indicate the constant C^s_{NaCl} and $C^s_{CaCl_2}$ systems, respectively. In B, ● and ○: $|J_{Na}/J_{Ca}|$, ■ and □: $|J_{Cl}/J_{Na}|$. In C, ● and ○: $C^m_{Na,Total}$, ▲ and △: $C^m_{Ca,Total}$.

Cl^- fluxes increased with decreasing Na^+ concentrations. It can be recognized that the ion transport processes of the NaCl–$CaCl_2$ system with a highly permselective cation-exchange membrane shift from the $CaCl_2$ transporting process ($J_{Ca}=(1/2)J_{Cl}$, $J_{Na}=0$), through the Na–Ca transporting process ($J_{Na}=-2J_{Ca}$, $J_{Cl}=0$), and finally to the NaCl transporting process ($J_{Na}=J_{Cl}$, $J_{Ca}=0$), as an increase in the relative Na^+ concentration of the external phase.

These membrane transport characteristics should be a reflex of the Na^+ and Ca^+ concentration profiles within the membrane phase plotted in Fig. 4-C. The total Ca^{2+} concentration in membrane, $C^m_{Ca,Total}$, was kept at high and constant level throughout the external concentration range studied, while the total Na^+ concentration within membrane, $C^m_{Na,Total}$, varied from a low level at 1/100 of $C^m_{Ca,Total}$ to high level comparable with $C^m_{Ca,Total}$, with the external Na^+ concentration change. In the limits of the $C^m_{Na,Total}/C^m_{Ca,Total}$ values from 1/20 ($C^s_{NaCl}/C^s_{CaCl_2}=1/10$) to 1/2 ($C^s_{NaCl}/C^s_{CaCl_2}=10$), the membrane process was controlled only by cations, Na^+ and Ca^{2+}. The Na^+ concentrations within the membrane phase increased with increasing external Na^+ concentrations, and finally reached at the same level as the membrane Ca^{2+} concentration when the external solution contained Na^+ in 30 times of Ca^{2+} concentration. The results given in Figs. 4-B and C suggest that, in the membrane utilizing techniques where the permeations of bivalent cation have to be avoided as far as possible, such as in the desalination process of sea water, the membrane concentration of bivalent cation should be kept, at least, not exceeding ca. 75% of the total membrane cations. Such a condition can be realized, in case of the CK-1, 1.0t cation-exchange membrane, by keeping the external bivalent cation concentrations at below 1/20 of the univalent cation concentrations.

Membrane/Solution Distribution of Cations and Membrane Transport Parameters. The ion concentration profiles within charged membrane phase, as an origin of the generation of a variety of the membrane transport phenomena, were discussed further in terms of the membrane transport parameters. As pointed out already, the NaCl–CsCl system with the CK-1, 1.0t membrane can be characterized as a cationic equilibrium system, in which the oppositely running Na^+ and Cs^+ fluxes with almost the same magnitudes were observed. And, accordingly the membrane potential responses are recognized as an ideal equilibrium potential for Na^+ and Cs^+ showing the linear relationships against the logarithmic external activity, $\log a^I_{M_i}$, with the slope of 59.16 mV predicted from Eq. 6. In these situations, the P_{Na}/P_{Cs} values calculated based on the electrochemical data are almost constant at 0.72 corresponding with the ideal value calculated based on Eq. 6 as shown in Fig. 5-A. A slight deviation of P_{Na}/P_{Cs} values from the ideal value was observed: the substantial negative and positive deviations were recognized in the higher and lower C^s_{NaCl}/C^s_{CsCl} regions, respectively, where the gradient of the membrane potential vs. logarithmic activity curves decreases similarly as illustrated in Fig. 3-A. These results were caused partly from the Cl^- transport across the membrane at quite low levels.

On the other hand, the Cl^- transport process was involved considerably in the ion transport phenomena across the CK-1, 1.0t membrane for the NaCl–$CaCl_2$ system as discussed above. In Fig. 5-B1, the P_{Na}/P_{Ca} values estimated from the electrochemical data are plotted and compared with those, indicated by the solid curve, evaluated from Eq. 6 providing that the observed transmembrane potentials correspond to the cationic equilibrium potential $V_{Na\text{-}Ca}$. For the potential responses illustrated in Fig. 4-A, the P_{Na}/P_{Ca} values, calculated from Eq. 6 with the condition of $P_{Cl}=0$, no longer give a constant value for the whole concentration ranges studied. When the system was characterized by only the cation transport process, the constant P_{Na}/P_{Ca} values were obtained as in the NaCl–CsCl system. As can be seen in Fig. 5-B1, a large positive deviation of the P_{Na}/P_{Ca} values from those evaluated by Eq. 6 are observed in the system with high $C^s_{NaCl}/C^s_{CaCl_2}$ ratio,

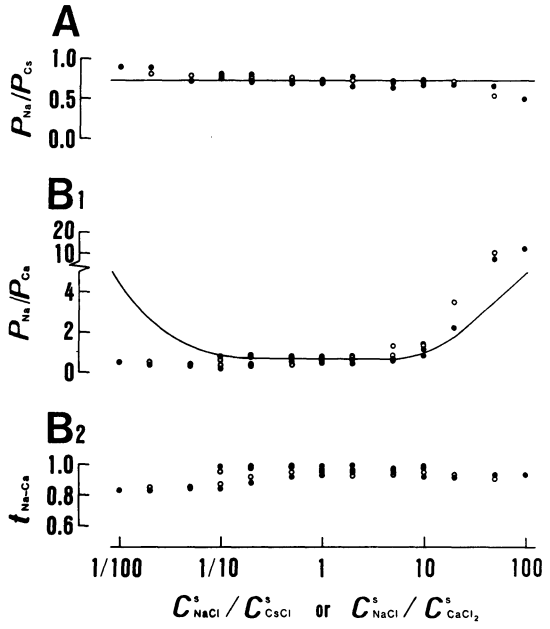

Fig. 5. Membrane permeability ratios, P_{Na}/P_{Cs} (A) and P_{Na}/P_{Ca} (B1), and transport number to whole cation, $t_{Na\text{-}Ca}$ (B2), as a function of the external NaCl/CsCl or NaCl/$CaCl_2$ concentration ratio, C^s_{NaCl}/C^s_{CsCl} or $C^s_{NaCl}/C^s_{CaCl_2}$. Closed marks indicate the constant C^s_{NaCl} system and open marks indicates the constant C^s_{CsCl} (A) or constant $C^s_{CaCl_2}$ (B1 and 2) systems.

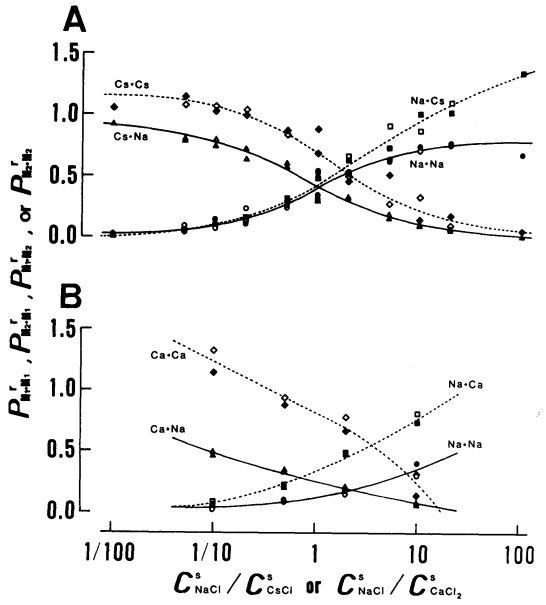

Fig. 6. Membrane permeability matrix elements as a function of the external electrolyte concentration ratio, C^s_{NaCl}/C^s_{CsCl} or $C^s_{NaCl}/C^s_{CaCl_2}$. Closed marks indicate the constant C^s_{NaCl} system and open marks indicate the constant C^s_{CsCl} (A) or constant $C^s_{CaCl_2}$ (B) systems. ● and ○: $P^r_{M_1,M_1}$ ▲ and △: $P^r_{M_2,M_1}$, and ■: and □ $P^r_{M_1,M_2}$, ◆ and ◇: $P^r_{M_2,M_2}$.

where the transport process can be characterized by the NaCl transport with small Ca^{2+} flux. On the other hand, in the low $C^s_{NaCl}/C^s_{CaCl_2}$ systems where the transport process can be characterized by the $CaCl_2$ transport with small Na^+ flux, the P_{Na}/P_{Ca} values kept at relatively constant level and a large negative deviation from the values based on Eq. 6 was observed. To examine further the influence of Cl^- permeation on the transport process across a cation-exchange membrane, the transport number to whole cation, Na^+ and Ca^+, $t_{Na\text{-}Ca}$, relative to t_{Cl} was evaluated in the NaCl-$CaCl_2$ systems. As shown in Fig. 5-B2, the $t_{Na\text{-}Ca}$ values decrease in these systems and there is a substantial effect of Cl^- transport on the cation transport.

When the membrane transport processes are controlled only by two cationic species, M_1 and M_2, the 3×3 membrane permeability matrix in Eq. 1 can be reduced to the 2×2 matrix describing the partial contributions of the inter-cationic correlations on the membrane process.[4,5] Figure 6 summarizes the elements of the 2×2 membrane permeability matrix for the NaCl-CsCl and NaCl-$CaCl_2$ systems estimated from the electrochemical and inter-compartmental ion flux data with the nonequilibrium thermodynamic relations discussed earlier. For the NaCl-$CaCl_2$ system, the permeability matrix element calculations were available only for the system in which Cl^- flux is negligible. In Fig. 6, the permeability matrix elements are plotted as a relative value against the membrane permeability to whole cation, $P_{M_1\text{-}M_2}$, as:

$$P^r_{M_1\cdot M_1} = P_{M_1\cdot M_1}/P_{M_1\text{-}M_2},\quad P^r_{M_1\cdot M_2} = P_{M_1\cdot M_2}/P_{M_1\text{-}M_2} \qquad (10)$$
$$P^r_{M_2\cdot M_1} = P_{M_2\cdot M_1}/P_{M_1\text{-}M_2},\quad P^r_{M_2\cdot M_2} = P_{M_2\cdot M_2}/P_{M_1\text{-}M_2}$$

Magnitudes of the membrane permeability matrix element driven by the electrochemical activity difference of some cations (see Eq. 1) increased with increasing relative concentration of those cations. The membrane permeability matrix representations including the Cl^- relating components were discussed in earlier papers of this series for the NaCl-$CaCl_2$ systems.[5]

Membrane/Solution Distribution and Diffusion of Cations within Membrane Phase. It has been an established concept based on the theoretical and experimental investigations of the membrane transport phenomena that the ion permselectivity of a charged membrane can be determined as a function of the migration speed of ions within the membrane phase and of the membrane/solution distribution coefficient of permeating ions. As a conclusion of the present experiments, the diffusion coefficient ratio of cations, $D^m_{M_1}/D^m_{M_2}$, and the cation concentration ratio, $C^m_{M_1,Total}/C^m_{M_2,Total}$, in the CK-1, 1.0t membrane phase are examined as a function of the external electrolyte concentration ratio, $C^s_{M_1Cl_1}/C^s_{M_2Cl_2}$. The results are summarized in Fig. 7. These two quantities are

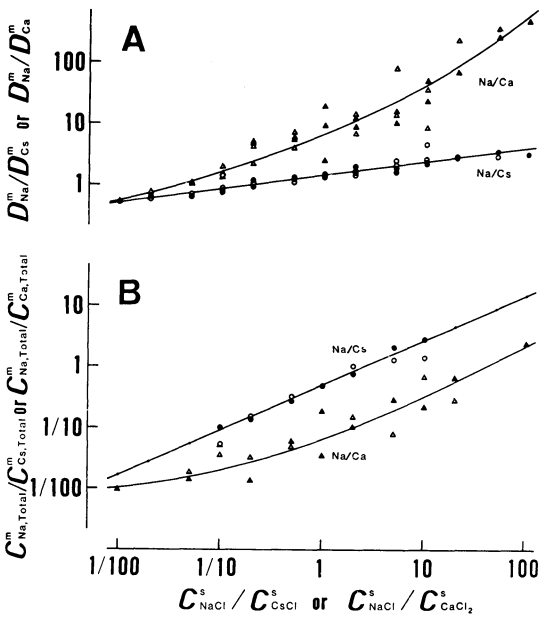

Fig. 7. Diffusivity ratio (A), D^m_{Na}/D^m_{Cs} or D^m_{Na}/D^m_{Ca}, and total cation concentration ratio (B), $C^m_{Na,Total}/C^m_{Cs,Total}$ or $C^m_{Na,Total}/C^m_{Ca,Total}$, within the membrane phase as a function of the external concentration ratio, C^s_{NaCl}/C^s_{CsCl} or $C^s_{NaCl}/C^s_{CaCl_2}$. Closed marks indicate the constant C^s_{NaCl} system and open marks indicate the constant C^s_{CsCl} or C^s_{CaCl} systems. ● and ○ refer to Na/Cs ratios, and, ▲ and △ refer to Na/Ca ratios.

important as a controlling factor to the membrane permselectivity in the multi-ionic systems. In case of the NaCl–CsCl system, in which all the permeating cations are univalent, the Na/Cs diffusivity ratio within the membrane phase was kept at an almost constant level, whereas the Na/Cs concentration ratio changed considerably corresponding with the changes in external Na/Cs concentration ratio. When bivalent cations were introduced as permeating species as in the NaCl–$CaCl_2$ system, the Na/Ca diffusivity ratio varied considerably, from 0.5 to 500, as compared with that of the NaCl–CsCl system. As mentioned before, at the upper or lower limilts of the Na/Ca diffusivity ratios, the systems were characterized by the NaCl or $CaCl_2$ transport process. Changes in the Na/Ca membrane concentration ratio within the membrane phase, on the other hand, were depressed to the limits not exceeding 100 times against the 10000 times changes in the external Na/Ca concentration ratio, from 1/100 to 100.

In the multi-ionic system with a highly permselective ion exchange membrane, the membrane transport process can be characterized as a function of the external electrolyte composition when the charges of counterions are the same. When the system contains the counterions with different charges, the membrane transport process tends to be controlled by the counterions with higher charges based on the monopolistic occupation of the available ion-exchange sites of membrane with multivalent counterions.

The authors wish to thank Asahi Chemical Industry Co., Ltd. for providing the ion-exchange membrane, CK-1, 1.0t, used in the present investigation. One of the authors (K. K.) is grateful to the Ministry of Education, Science and Culture for a Grant-in-Aid for Scientific Research on Priority Areas and to the Kurata Foundation for the research grant support.

References

1) F. Helfferich, "In Exchange," McGraw-Hill, New York (1962).
2) N. Lakshminarayanaiah, "Transport Phenomena in Membranes," Academic Press, New York (1969).
3) M. E. Starzak, "The Physical Chemistry of Membranes," Academic Press, Orlando, Florida (1984).
4) K. Kaibara and H. Kimizuka, *Bull. Chem. Soc. Jpn.*, **55**, 1743 (1982).
5) K. Kaibara, H. Inoue, and H. Kimizuka, *Bull. Chem. Soc. Jpn.*, **60**, 3175 (1987).
6) V. S. Soldano and V. A. Bychkova, *Russ. J. Phys. Chem.*, **44**, 1297 (1970).
7) M. A. Lake and S. S. Melsheimer, *AIChE J.*, **24**, 130 (1978).
8) R. Smith and E. Woodburn, *AIChE J.*, **24**, 577 (1978).
9) M. J. Manning and S. S. Melsheimer, *Ind. Eng. Chem., Fundam.*, **22**, 311 (1983).
10) K. Kaibara, K. Saito, and H. Kimizuka, *Bull. Chem. Soc. Jpn.*, **46**, 3712 (1973).
11) K. Kaibara, H. Inoue, S. Tsuruyama, and H. Kimizuka, *Bull. Chem. Soc. Jpn.*, **61**, 1517 (1988).
12) H. Kimizuka and K. Kaibara, *J. Colloid Interface Sci.*, **52**, 516 (1975).
13) H. Kimizuka, K. Kaibara, E. Kumamoto, and M. Shirozu, *J. Membrane Sci.*, **4**, 81 (1978).